Three-Dimensional Structure of the Reduced C77S Mutant of the *Chromatium vinosum* High-Potential Iron−Sulfur Protein through Nuclear Magnetic Resonance: Comparison with the Solution Structure of the Wild-Type Protein[†,‡]

Detlef Bentrop,[§] Ivano Bertini,*[,§] Francesco Capozzi,[||] Alexander Dikiy,[§] Lindsay Eltis,[⊥] and Claudio Luchinat[||]

Department of Chemistry, University of Florence, Via Gino Capponi 7, 50121 Florence, Italy, Institute of Agricultural Chemistry, University of Bologna, Viale Berti Pichat 10, 40127 Bologna, Italy, and Department of Biochemistry, Université Laval, Québec City, Québec G1K 7P4, Canada

Received December 4, 1995; Revised Manuscript Received February 15, 1996[⊗]

ABSTRACT: The full ^{1}H NMR assignment of the reduced C77S mutant of *Chromatium vinosum* high-potential iron−sulfur protein (HiPIP) was achieved by taking advantage of the assignment available for the wild-type protein. A total of 1565 nuclear Overhauser effect (NOE) spectroscopy cross peaks were integrated and converted into distance constraints, of which 497 were found to be irrelevant. An additional 24 dipolar constraints were obtained from one-dimensional NOE difference spectra by saturating hyperfine-shifted βCH_2 cysteine/serine protons. Forty-six $^3J_{NH-H\alpha}$ coupling constants and eight hydrogen bonds provided further constraints. Through a distance geometry approach, a family of 15 structures was calculated, which was subsequently subjected to restrained energy minimization. The root mean square deviations of the minimized structures were 0.62 ± 0.09 and 1.09 ± 0.11 Å for backbone and heavy atoms, respectively. The resulting solution structures are very similar to those of the reduced wild-type protein (WT). An analysis of the NOEs experienced by the protons of Ser-77 in both the reduced and oxidized forms reveals that they are very similar to those experienced by Cys-77 in WT. On the basis of the hyperfine shifts observed for the Ser-77 protons and of the present structural analysis, it is concluded that the serine O_γ atom is coordinated to the polymetallic center, thus confirming the strict analogy of the electronic structures of the polymetallic center in both proteins. Capillary electrophoresis experiments demonstrate coordination of Ser-77 as an anion. Serine *versus* cysteine coordination in iron-sulfur proteins is briefly discussed.

High-potential iron−sulfur proteins (HiPIPs)[1] are a class of proteins which contain one Fe_4S_4 cluster and span a range of reduction potentials from +450 to +50 mV (Meyer et al., 1983). They are generally found in phototrophic purple bacteria (Bartsch, 1978). Their Fe_4S_4 cluster passes from net charge +3 to +2 during the electron transfer process in which these proteins are involved (Carter et al., 1972). HiPIPs differ from other Fe_4S_4-containing electron transfer proteins such as ferredoxins in both the accessible cluster charges, which in ferredoxins are +2 to +1, as well as their positive reduction potentials, which in ferredoxins are as low as −600 mV (Yoch & Carithers, 1979; Armstrong et al., 1988). It has been suggested that these differences between HiPIPs and ferredoxins can be explained by different partial charges of the polypeptide moieties [particularly by the dipoles generated in peptide bonds between the negatively charged carbonyl oxygen and the positively charged NH hydrogen (Jensen et al., 1994)]. On the other hand, differences in reduction potential between HiPIPs have been ascribed principally to differences in net protein charges due to ionized surface residues (Banci et al., 1995).

In the framework of an investigation of the molecular factors determining the macroscopic redox potential of Fe_4S_4 electron transfer proteins, we have studied the C77S variant of *Chromatium vinosum* HiPIP, in which the fourth cysteinyl cluster ligand is replaced by a serine residue. Over the pH range of stability, which is similar to that of WT, its reduction potential is 25 mV lower (330 mV *versus* 355 mV for WT) (Babini et al., 1996). This observation is consistent with the expected and observed decrease of redox potential of FeS clusters after replacement of a coordinating cysteine by a serine [Kowal et al. (1995) and references therein], since oxygen coordination would preferentially stabilize the oxidized form of the cluster because of its larger electronegativity. The C49S mutant of *Anabaena* 7120 vegetative Fe_2S_2 ferredoxin with a reduction potential that is ca. 100 mV higher than that of the wild-type ferredoxin is a remarkable exception (Cheng et al., 1994). In the present case, the reduction of the redox potential is significantly lower than the 60- and 72-mV decrease measured for the low-potential $[Fe_4S_4]^{2+,1+}$ clusters in the C148S and C151S mutants of *Escherichia coli* fumarate reductase, respectively (Kowal et al., 1995).

[†] This work is partially supported by Progetto Finalizzato Biotecnologie, Comitato Biotecnologie, and Comitato Scienze Agrarie of CNR, Italy.

[‡] The coordinates for the family of 15 NMR structures have been deposited in the Brookhaven Protein Data Bank under the file name 1NOE.

* Corresponding author.
[§] University of Florence.
[||] University of Bologna.
[⊥] Université Laval.

[⊗] Abstract published in *Advance ACS Abstracts,* April 1, 1996.

[1] Abbreviations: NMR, nuclear magnetic resonance; 1, 2 D, one-, two-dimensional; NOE, nuclear Overhauser effect; NOESY, nuclear Overhauser effect spectroscopy; TOCSY, total correlation spectroscopy; DG, distance geometry; REM, restrained energy minimization; RMSD, root mean square deviation; HiPIP, high potential iron−sulfur protein; WT, wild-type protein; CE, capillary electrophoresis.

S0006-2960(95)02851-0 CCC: $12.00

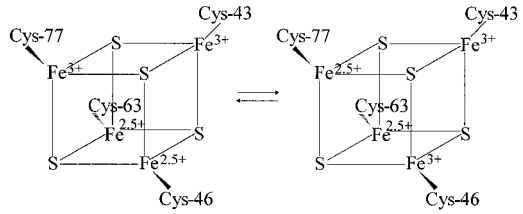

FIGURE 1: Schematic representation of the equilibrium between two species in oxidized HiPIP from *C. vinosum*.

Oxidized HiPIP clusters exhibit a complex behavior in terms of valence distribution among the iron ions (Banci et al., 1993). The oxidized HiPIP from *C. vinosum* has been proposed to experience an equilibrium between two species of the type shown in Figure 1, where the two species differ in the positions of the mixed-valence and ferric pair. The WT protein has 60% of the right isomer, whereas the C77S mutant has 40% of the same isomer. This is the effect of replacing one of the cluster-coordinating cysteine residues by a serine (Babini et al., 1996).

We report here the solution structure of the reduced C77S HiPIP from *C. vinosum* in order to investigate both the type of binding of the serine residue to the cluster and the conformations of the cluster-coordinating amino acids and the protein backbone. The three-dimensional structure determination of a Fe_4S_4 electron transfer protein with a cysteine to serine mutation in the cluster ligand sphere is unprecedented. Since ^{1}H NMR is not able to provide direct information on the Fe_4S_4 polymetallic center, the cluster has been assumed to be equal to that of WT.

EXPERIMENTAL PROCEDURES

NMR Sample and Experiments. All chemicals used were of the best quality available. The C77S mutant of *C. vinosum* HiPIP was expressed in *E. coli* and purified as described earlier (Babini et al., 1996). The protein is stable in the reduced state. Samples for NMR spectroscopy contained the C77S HiPIP mutant at a concentration of 4−5 mM in 50 mM sodium phosphate buffer/50 mM NaCl, pH 7.0, or in 50 mM sodium phosphate buffer, pH 5.1 (either in H_2O or in D_2O). The 100-ms NOESY spectrum at 290 K, from which almost all distance constraints for the structure calculation were derived, was recorded in H_2O in the latter buffer.

One-dimensional spectra, 1D NOE difference, 2D NOESY, and TOCSY ^{1}H NMR experiments were performed on a Bruker AMX spectrometer operating at 600.14 MHz proton Larmor frequency in a fashion analogous to those for reduced WT (Banci et al., 1995). To ensure the achieved assignments, the experiments were carried out at both 290 and 303 K.

Capillary Electrophoresis. Capillary electrophoresis (CE) runs were performed on a Biofocus 3000 instrument (Bio-Rad) using a coated Bio2 column (Bio-Rad; 24 cm × 25 μm). The column was equilibrated and proteins were eluted with borate buffer (pH 8.65) at 293 K. A constant voltage of 8 kV (10-μA current) has been applied. Absorbance was detected at 254, 280, and 350 nm.

Structure Calculations. For the computation of the structure, volumes of assigned NOESY cross peaks were processed according to the methods described earlier for reduced WT (Banci et al., 1995). As in the latter case, the standard distance geometry (DG) calculations were supplemented by extensive use of the redundant dihedral angle strategy (REDAC) (Güntert & Wüthrich, 1991) for the definition of starting conformations.

In order not to impose the geometry of the Ser-77 side chain by bonding its O_γ to one of the cluster Fe atoms, the Fe_4S_4 cluster was constructed in the following way: two artificial amino acids were added to the residue library of the DIANA program package. The first one is the same as that used for the construction of a Fe_4S_4 cluster in native HiPIPs with 4-fold cysteinyl ligation of the cluster (Banci et al., 1995). It consists of a cysteinyl residue in which the thiol hydrogen (H) was replaced by an iron atom (Fe) at the proper distance which in turn is bound, through another covalent bond, to the sulfur atom (S) that constitutes the "inorganic" sulfide in the cluster. This residue can be described by the formula Cys−S_γ−Fe−S. Bond lengths and angles used in constructing this residue were derived from the average of these parameters observed in known X-ray structures of HiPIPs (Carter et al., 1974; Breiter et al., 1977; Benning et al., 1994; Rayment et al., 1992). The second artificial residue for the C77S variant was obtained from the former by adding yet another covalently bonded -Fe−S moiety. Thus, it is represented by the formula Cys−S_γ−Fe−S−Fe−S. Bond lengths and angles for the second residue were also obtained from the average of these parameters in known X-ray structures of HiPIPs.

Two modified cysteines of the first type (Cys-46 and Cys-63) and one modified cysteine of the second type (Cys-43) can mimic the geometry of the cluster if the four iron atoms and the four "inorganic" sulfur atoms (S) are linked through covalent bonds along the edges of the cubane. Five of these bonds [as opposed to four in the case of WT (Banci et al., 1995)] belong to the artificial residues, and seven are treated by DIANA as "special covalent bonds" after defining the appropriate upper and lower distance limits. Additional "special covalent bonds" were introduced to maintain the shape of the cube, as described earlier (Banci et al., 1995). A total of 23 links, which are analogous to those employed in the case of WT, were used. In this manner, a rigid cluster can be defined, leaving at the same time undefined the chirality of the peptide folding around it.

The Ser-77 residue was assumed to be deprotonated; therefore, a serinate residue without the hydroxyl hydrogen was added to the residue library of DIANA. All new residue entries in the DIANA library are available as supplementary material. The distance between O_γ of Ser-77 and its closest iron atom (the second iron atom of the modified Cys-43) was loosely restrained to 1.50−2.50 Å by introducing the corresponding lower and upper distance limits. Moreover, in analogy to WT, the distances between Ser-77 O_γ and the S_γ atoms of Cys 43, Cys-46, and Cys-63 were restrained to 6.00−6.38 Å (the corresponding lower and upper distance limits are a subset of those necessary to maintain a rigid cluster). No restrictions were applied for the angle C_β−O_γ−Fe. In the very last run of DIANA the interresidual upper distance limits for Hβ_1 of Ser-77 were supplemented by the corresponding lower distance limits, while all upper and lower distance limits involving the O_γ of Ser-77 (including its van der Waals radius) were removed to allow the latter atom to establish its position without artificial constraints. The subsequent REM calculations were also carried out without distance limits for Ser-77 O_γ.

Hydrogen Bond Constraints. The threshold values to define a hydrogen bond in DG calculations were 2.40 Å for

FIGURE 2: Scheme of the sequential connectivities involving NH, Hα, and Hβ protons in the reduced C77S-HiPIP from *C. vinosum* obtained through standard 2D NMR experiments. Dipolar NH−Hα connectivities are divided into strong (thick lines) and weak (thin lines). Filled squares indicate slowly exchanging NH protons.

the H···O distance and ± 35 degrees of deviation from linearity for the N···H···O angle. A hydrogen bond was introduced as a constraint for DG calculations only if the amide proton was observed in D_2O solution and if the hydrogen bond involving that amide proton was observed in more than 70% of the structures generated as output of successive runs. An upper distance limit of $r_{H\cdots O} < 2.40$ Å was applied for each hydrogen bond. The N···O distance was constrained to lie between 2.60 and 3.30 Å.

Backbone Dihedral Angle Constraints. A NOESY spectrum recorded with a mixing time of 100 ms was zero-filled to give a 8 K × 1K data point matrix from which information on the $^3J_{NH-H\alpha}$ coupling constants was extracted. The program INFIT (Szyperski et al., 1992) was used to fit the line shape of cross peaks involving NH protons. A redundant angle constraints file was used to select among the possible allowed intervals for the ϕ dihedral angles. To account for the inaccuracy of the measured J values, the corresponding ϕ angle was loosely restrained to $\phi \pm 30°$.

As in the case of WT, the distance geometry calculations were supplemented by restrained energy minimization (REM) on the 15 structures of the DG family with the lowest target function values (Banci et al., 1995). In the REM calculations, improved partial charges (Mouesca et al., 1994) were used for the iron and sulfur atoms as well as the iron-bound cysteines. All other force field parameters were the same as previously reported for WT protein. For the O_γ atom of Ser-77, the force field parameters of the cysteine S_γ atoms were used.

The analysis of NMR spectra and all DG and REM calculations (double-precision accuracy) were performed on IBM RISC 6000/530 computers.

RESULTS AND DISCUSSION

Proton Assignment. An extensive assignment of the proton resonances of the reduced C77S HiPIP was established in a straightforward manner, taking advantage of the extended proton assignments for the reduced and oxidized WT HiPIPs (Gaillard et al., 1992; Banci et al., 1995; Bertini et al., 1995).

Most of the spin systems were identified from 2D TOCSY experiments recorded with a mixing time of 80 ms in both H_2O and D_2O solutions. In total, 70 spin systems were identified from these experiments. The sequence-specific assignment was performed following the standard method developed by Wüthrich and others (Wüthrich, 1986; Arseniev et al., 1988; Schultze et al., 1988). The comparative analysis of 2D NOESY and TOCSY maps allowed us to detect sequential connectivities (Figure 2) of 74 amino acids (Ala-0−Ala-2, Pro-3−Tyr-19, Asn-20−Arg-33, Pro-34−Leu-36, Pro-38−His-42, Ala-44−Asn-45, Gln-50−Cys-63, Gln-64−Leu-65, Pro-67−Gly-75, and Thr-81−Gly-85). The pattern of these sequential connectivities is very similar to that reported for WT (Banci et al., 1995), thus already indicating close overall structural similarity of the two proteins.

Of the 70 amino acids whose spin systems were identified, 67 were also sequentially assigned. The remaining amino acids were assigned on the basis of similar connectivities as

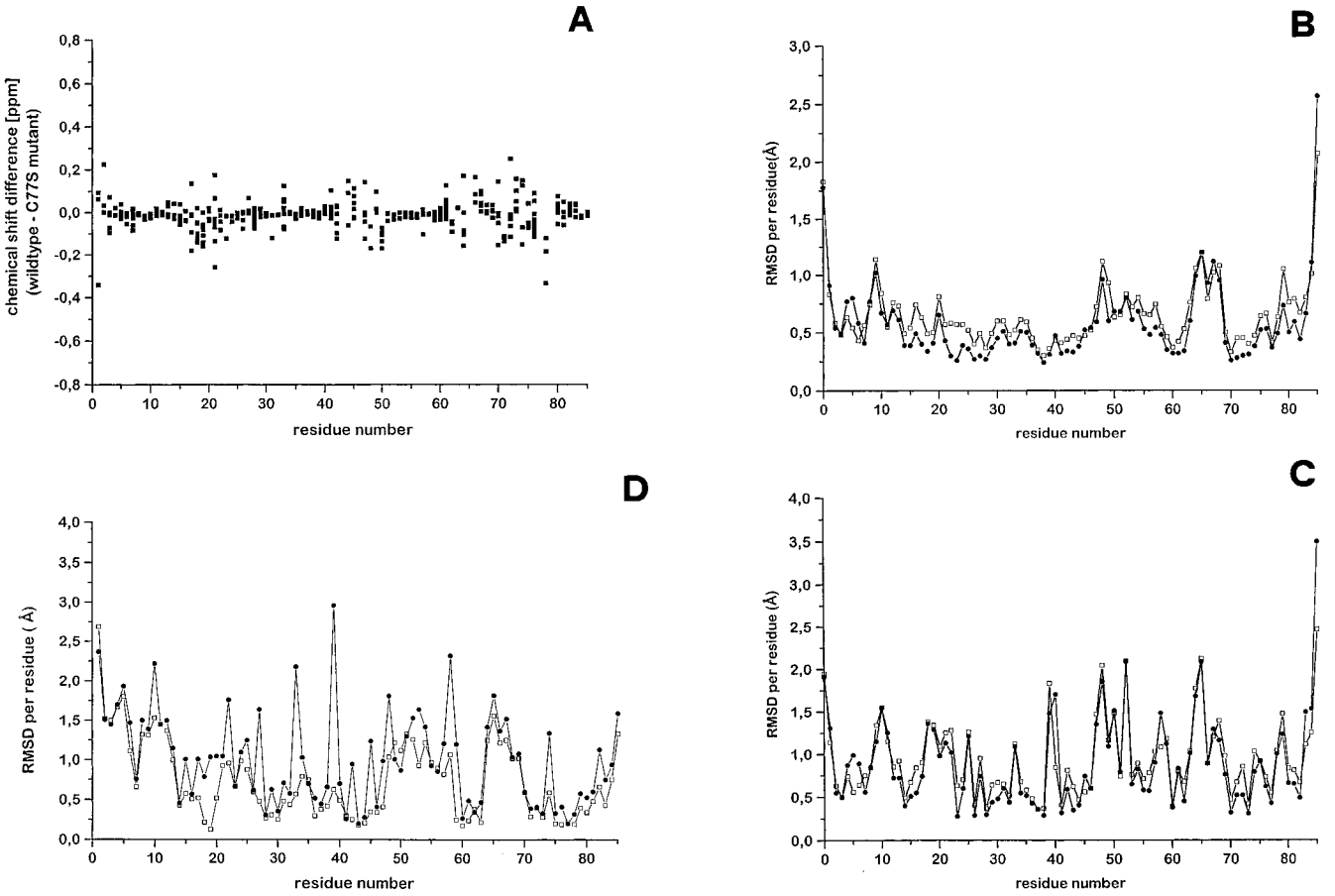

FIGURE 3: (A) Chemical shift differences of all assigned ^{1}H nuclei on passing from the reduced WT to the C77S mutant of the HiPIP from *C. vinosum*. The individual differences for each assigned proton are plotted versus the residue number. The proton resonances of the cluster ligands (Cys-43, Cys-46, Cys-63, Cys/Ser-77) are not taken into consideration. (B, C) Diagrams of the RMSD per residue for the 15 accepted structures of the reduced C77S HiPIP from *C. vinosum* after DG (□) and REM (●) calculations. RMSD values for the backbone and the heavy atoms are presented in panels B and C, respectively. (D) Diagram of the RMSD per residue for the mean structures of the reduced C77S and WT HiPIP from *C. vinosum* at REM level. RMSD values for the heavy atoms (●) and the backbone (□) are given.

in the WT. Identification of the spin patterns of the cluster-coordinating cysteines and Ser-77 and their sequence-specific assignment were achieved by 1D NOE experiments (Bertini et al., 1992) as reported previously (Babini et al., 1996).

In summary, 85 out of 86 amino acids were completely or partially assigned; as in both reduced and oxidized WT, only Ser-79 remained unassigned. In WT, the backbone amide proton of the latter residue forms a hydrogen bond with the sulfur atom of Cys-77 (Backes et al., 1991). Thus, the proximity of residue 79 to the FeS center and concomitantly strongly enhanced nuclear relaxation may explain why it escaped detection.

A total of 422 protons were assigned, which corresponds to 87% of the protons in the protein. These numbers are very similar to those obtained for WT. The ^{1}H NMR assignment of the reduced recombinant C77S *C. vinosum* HiPIP mutant obtained in this work is summarized in the supplementary material.

The proton chemical shifts of the reduced WT and C77S mutant of *C. vinosum* HiPIP are very similar in most cases. Figure 3A presents the differences of the ^{1}H chemical shifts on a per-residue basis for the two proteins. The resonances of the cluster-coordinating residues are not taken into consideration. None of the chemical shift differences exceed 0.4 ppm; thus, they are considerably smaller than the differences observed between reduced and oxidized WT (Bertini et al., 1995). It is, however, worth noting that the sequential stretches with the largest chemical shift differences are the same in both cases and are in the spatial vicinity of the cluster, the only exception being the modified N-terminus of the C77S mutant.

Structure Determination. A total of 1565 upper distance constraints were obtained after analysis of NOESY spectra and after running the CALIBA program (Güntert et al., 1991). Twenty-four additional dipolar connectivities were determined from 1D NOE difference spectra recorded upon saturation of the hyperfine-shifted signals. The constraints constituting the upper distance limits are summarized in Table 1, which also provides the upper distance limits corresponding to the eight hydrogen bonds that were introduced during the course of the structure computations. The distance geometry program DIANA (Güntert et al., 1991) found 497 of these constraints to be redundant for the structure determination, i.e., either no conformation of the peptide chain could give rise to violations of these constraints or they belong to fixed proton−proton distances. Thus, 1092 distance constraints were used for the structure calculation, which is similar to the number of meaningful constraints used for the structure determination of WT.

From cross peaks involving NH protons whose line widths were typically between 7 and 20 Hz (average error of the line width fit: 0.8 ± 0.4 Hz), 46 $^3J_{\text{NH-H}\alpha}$ coupling constants were determined and translated into ϕ dihedral angle constraints. Initial DIANA runs were carried out without these restraints. Inspection of the angle constraints file after these initial runs revealed that the ϕ angle constraints in

Table 1: Number of Constraints Constituting the Upper Distance Limits File for the Reduced C77S HiPIP and for the Reduced and Oxidized WT HiPIP from *C. vinosum*

class	definition	number of NOESY cross peaks (methyl peaks)		
		reduced C77S	reduced WT	oxidized WT
1	intraresidue (except NH, Hα, Hβ)	384 (62)	344 (59)	370 (70)
2	sequential and intraresidue (NH, Hα, Hβ)	486 (67)	459 (62)	477 (67)
3	medium range	110 (16)	105 (14)	105 (14)
4	long range backbone	31	27	32
5	long range	554 (214)	554 (195)	553 (219)
	total number of upper distance limits from CALIBA	1565	1489	1537
	additional upper distance limits from 1D-NOEs	24	28	39
	additional upper distance limits from hydrogen bonds	16 (8 H-bonds)		
	total number of meaningful distance constraints	1092	1147	1142

this file were already more restrictive than the *J*-derived constraints in most cases. However, this was not the case for Ser-1, Leu-17, Ala-23, Thr-24, and Glu-59, for which the angle constraints file was thus supplemented with the respective *J*-derived ϕ angle constraint. Sixty-two stereospecific assignments were obtained by using the program GLOMSA (Güntert et al., 1991).

It has been reported that the chemical shifts of the hyperfine-shifted proton resonances can be used to derive the Fe−S−C_β−H dihedral angles for cluster-ligating cysteines in Fe_4S_4 proteins by means of a Karplus-type relationship (Bertini et al., 1994; Davy et al., 1995). This relationship may not hold in the present case because its coefficients were derived from data on proteins with 4-fold cysteine ligation of the 4Fe cluster. Consequently, no dihedral angle constraints for the cluster ligands of the C77S mutant were used during the structure calculation.

The three-dimensional structure of the reduced recombinant C77S *C. vinosum* HiPIP mutant was derived in two steps: distance geometry calculations (DG), using the already mentioned program DIANA, and restrained energy minimization (REM), by means of the AMBER 4.0 program package (Pearlman et al., 1991). More than 2000 random DIANA structures have been computed and a total of 24 REDAC cycles were carried out to generate redundant angle constraints (Güntert & Wüthrich, 1991). During all calculations, distance constraints were applied. Primary NOEs were used exclusively, although their intensities may be affected by spin diffusion, paramagnetic relaxation, and internal motions.

In analogy with the reduced WT, the DG family consisted of 15 structures produced by DIANA with the lowest target function ($\leq$0.50 Å^2) and residual violation of distance constraints not exceeding 0.2 Å. The distribution of the RMSD per residue inside the DG family for both backbone and heavy atoms is shown in Figure 3, panels B and C, respectively. The average values of the RMSD within the DG family are 0.71 $\pm$ 0.10 and 1.12 $\pm$ 0.12 Å for backbone and heavy atoms, respectively. The corresponding values for the reduced WT (0.73 $\pm$ 0.12 and 1.13 $\pm$ 0.12 Å, respectively) were not significantly different. Therefore, the quality of both families of structures is very similar.

As seen in Figure 3B,C, the distribution of the RMSD per residue for both backbone and heavy atoms has the same overall pattern as for WT [Figure 5 of Banci et al. (1995)]. The maximal RMSD values for backbone atoms are observed for the residues Phe-48 and Leu-65−Pro-67. This is due to the low number of NOEs for these amino acids, as is true for the reduced WT. An additional RMSD maximum not present in the reduced WT is found in the region of Ala-9. The average RMSD value for the N-terminal half of the protein is much lower than that of the C-terminus.

REM calculations lead to a decrease of the RMSD per residue with respect to the DG family as clearly seen in Figure 3B,C. The average values of the RMSD per residue within the REM family of structures are 0.62 $\pm$ 0.09 and 1.09 $\pm$ 0.11 Å for backbone and heavy atoms, respectively (the total energy for the REM family is -4955.2 kJ mol^{-1}). Compared to the corresponding values of 0.69 $\pm$ 0.11 and 1.14 $\pm$ 0.11 Å for the reduced WT, a more marked improvement of the quality of the structure can be observed. We note that the heavy-atom RMSD values for the amino acids Glu-40, Asp-52, and Asp-58 become higher after REM. Since these residues are well determined by dipolar connectivities, this finding and the high-heavy atom RMSD of Glu-39 are most likely due to mobility of their charged side chains on the surface of the protein. Relatively low values of the order parameter *S* (Hyberts et al., 1992) for the χ_1 dihedral angle confirm this notion in three of the four cases. Glu-40 displays a S(χ_1) value close to 1, indicating high order for the corresponding part of its side chain.

The DG and REM families of the C77S mutant are shown as stereo drawings in Figure 4. It can be seen that the structures of the DG and REM families are virtually identical, the lower RMSD of the REM family being reflected by an apparently increased resolution. As already mentioned, order parameters *S* were calculated to better evaluate the quality of the obtained structures. In general, the order parameters for the ψ and χ_1 dihedral angles reflect the distribution of the backbone and heavy-atom RMSD values, respectively. For the REM family, the lowest $S(\psi)$ values (i.e., the highest degree of disorder for the backbone) were found for the amino acids Ala-6, Asn-20, Cys-63, Gly-75, Ala-78, and Trp-80, thus confirming that the N-terminal half of *C. vinosum* HiPIP has a better defined structure than the C-terminal part. In the case of the χ_1 angle the same criterion identifies Asp-10, Glu-39, Gln-50, Asp-52, Asp-58, Gln-64, Leu-65, and Ser-79 as the amino acids with the most disordered side chains. For Gln-64, Leu-65, and Ser-79 this is clearly due to the paucity or, in the case of Ser-79, the complete lack of NOEs as a consequence of close spatial proximity to the cluster and therefore does not necessarily imply large mobility of these side chains. The mobility of the side chains of Asp-52 and Asp-58, which belong together with Gln-50 to an external loop of the protein, was discussed above. The residues of this loop show mainly sequential NOEs but only a few long-range NOEs to residues which are located exclusively toward the C-terminus of *C. vinosum* HiPIP.

Serine Coordination. One of the motivations of the current work was the question whether NMR can provide experi-

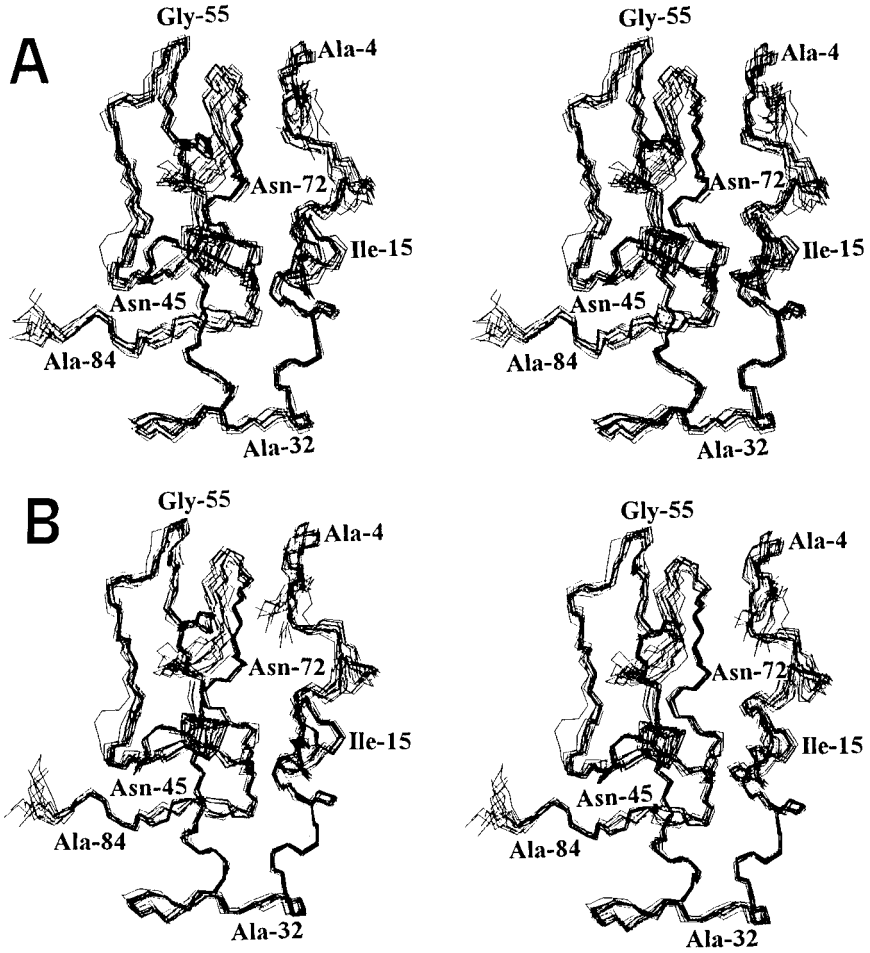

FIGURE 4: Stereo drawings of the 15 accepted structures of the reduced C77S HiPIP from *C. vinosum* obtained after DG (A) and REM (B) calculations.

Table 2: Overview of the Common 1D NOEs of Residue 77 in the Reduced and Oxidized WT and C77S Proteins[a]

	reduced WT		reduced C77S			
NOE	intensity (%)	distance (Å)	intensity (%)	distance (Å)	lol for DG (Å)	upl for DG (Å)
Hβ_1 77−Hβ Leu-17	3.41	2.6	1.44	2.7	2.4	2.7
Hβ_1 77−Hα Tyr-19 (ref)	2.93	2.7	1.38	2.7	2.4	2.7
Hβ_1 77−Hβ Tyr-19	1.41	3.1	1.45	2.7	2.4	2.7
Hβ_1 77−NH Ala-78	8.16	2.3	2.79[b]	2.4	2.6	3.1

	oxidized C77S		oxidized WT	
NOE	intensity (%)	distance (Å)	intensity (%)	distance (Å)
Hβ_1 77−Hβ Leu-17	6.92	2.8	4.18	2.8
Hβ_1 77−Hδ Leu-17	overlapped	−	0.54	3.9
Hβ_1 77−Hα Tyr-19 (ref)	7.78	2.7	4.77	2.7
Hβ_1 77−Hβ Tyr-19	overlapped	−	2.32	3.1
Hβ_1 77−NH Ala-78	7.94	2.7	6.45	2.6
Hβ_2 77−Hα Tyr-19 (ref)	6.20	2.7	10.29	2.7
Hβ_2 77−Hβ Tyr-19	3.86	2.9	4.94	3.1
Hβ_2 77−Hδ Tyr-19	4.02	2.9	4.75	3.1
Hβ_2 77−NH Ala-78	0.91	3.7	1.20	3.9
Hα 77−Hα Tyr-19 (ref)	7.14	2.2	5.90	2.2
Hα 77−Hϵ Trp-76	9.05	2.1	5.05	2.3
Hα 77−NH Ala-78	3.48	2.5	3.43	2.4

[a] The table also contains interresidual lower (lol) and upper distance limits (upl) for Hβ_1 Ser-77, which were used in the very last DG run of the structure calculation of the reduced C77S protein. [b] Overlap with Hα 77.

mental evidence of serine coordination to the Fe_4S_4 cluster. Coordination is strongly suggested by the observed hyperfine shifts of the Ser-77 protons, which compare well with those observed for the corresponding cysteine protons of WT in both oxidized and reduced species. The problem of serine coordination was further investigated by DG calculations without imposing serine coordination, as described under Experimental Procedures, and allowing the serine side chain to orient freely according to the experimental NOE constraints for Hβ_1 of Ser-77 (Table 2 and Figure 7B). The latter is the only proton of this residue on which steady-state 1D NOE experiments can be performed since it is hyperfine-shifted outside the diamagnetic region of the spectrum. Quantitative distance information from its neigh-

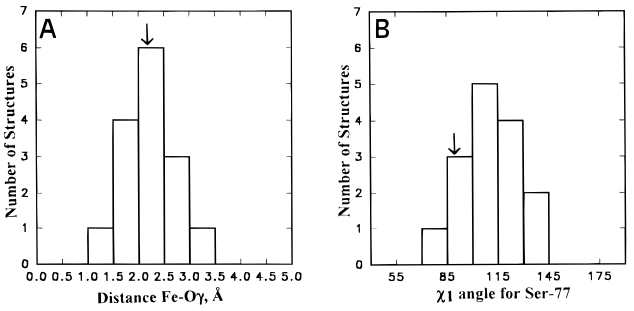

FIGURE 5: Histograms of the Fe−Oγ Ser-77 distances (A) and the χ1 dihedral angles of Ser-77 (B) for the 15 structures of the DG family of reduced C77S HiPIP from *C. vinosum*. The corresponding values for the X-ray structure of WT are indicated by arrows.

boring protons was thus obtained, which is, on the average, more accurate than NOESY data. In order to avoid internal calibration problems, the NOEs were compared with the analogous NOEs obtained from Hβ_1 of Cys-77 in WT, and the interproton distances were calibrated against the same reference NOE (Hβ_1 77−Hα 19) as in the native protein (Table 2). The similarity of these NOEs provides a preliminary indication that the χ_1 angles of Cys-77 and Ser-77 are very similar. Table 2 also contains the upper and lower distance limits for the very last DG run in which no link was imposed between the serine oxygen and any cluster or protein atom except the serine β-carbon. The family of 15 structures obtained from this DIANA run was examined for the distribution of χ_1 values and O−Fe distances. The results are shown in Figure 5. The χ_1 value (Figure 5B) is 111° ± 15°, close to the value of 89° found in WT, and the average O−Fe distance is 2.3 ± 0.6 Å (Figure 5A). Thus, it is concluded that serine coordinates to the Fe_4S_4 cluster. Considering that the Fe and O atoms cannot be monitored by NMR under the present experimental conditions, the obtained information is quite remarkable.

In the oxidized form both β-CH_2 protons and the α-CH proton of both Cys-77 and Ser-77 are shifted outside the diamagnetic region of the spectrum. These shifts have been interpreted within the context of the contact shifts in the series of oxidized HiPIPs. There are many NOEs from the β-CH_2 and α-CH protons to the surrounding protein protons, all of which are similar to those experienced by the analogous protons in the WT protein (Table 2). Therefore, although the structure of the C77S mutant in the oxidized form is not known, we can conclude that the serine residue is coordinated also in the oxidized form. The analysis of the hyperfine shifts had already indicated the similarity between the two proteins (Babini et al., 1996).

Capillary electrophoresis experiments were performed to investigate whether serine binds as neutral ligand or as serinate anion. Electrophoresis is in principle able to discriminate between quasi-identical proteins differing by a unit charge, as it would be the case between the present WT and mutant proteins if Ser-77 in the mutant were protonated. Therefore, we performed four CE runs of reduced and oxidized samples of WT and mutant proteins under otherwise identical conditions. For the reduced form of the C77S protein and WT the retention times were 6.64 ± 0.10 and 6.85 ± 0.10 min, respectively, while the oxidized C77S protein and WT were eluted after 7.64 ± 0.10 and 7.60 ± 0.10 min, respectively. These results demonstrate that the difference of one unit charge between oxidized and reduced forms is easily detected, whereas no difference is observed between WT and mutant. Thus, satisfactory discrimination was achieved between two different redox states of the same protein where the extra charge is on the cluster and approximately as internal as the one under consideration on ligand residue 77. Therefore, it has to be expected that a protonated serine would be equally well discriminated from a deprotonated cysteine. Since there is no discrimination between WT and mutant protein in the same redox state, it follows that Ser-77 is coordinated to the cluster as an anion. To our knowledge, this has not been demonstrated for any of the cysteine-to-serine mutations described in the literature

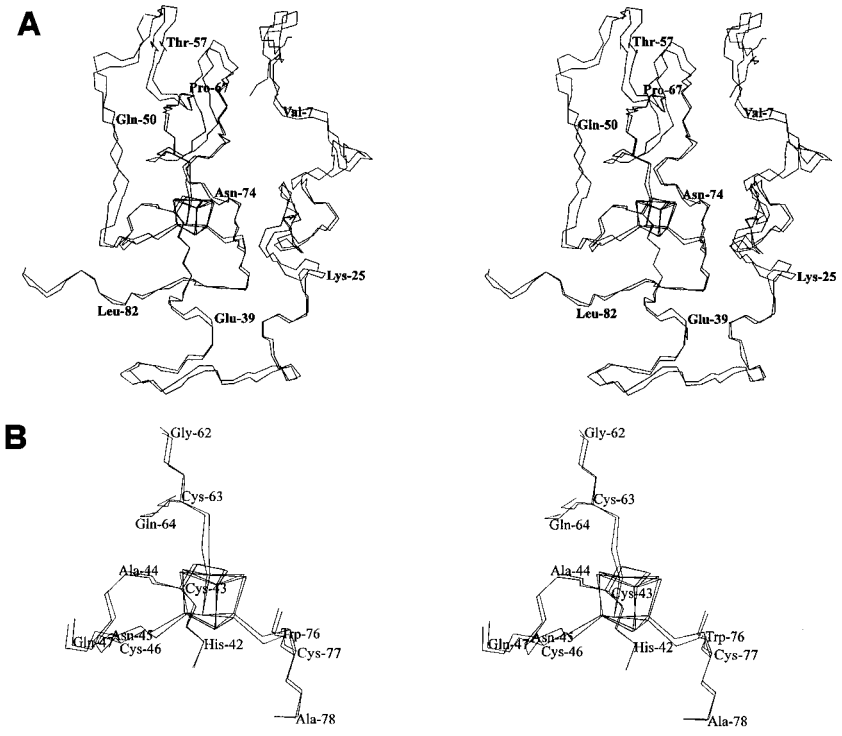

FIGURE 6: (A) Stereo drawings of the backbone atoms of the mean structures of the reduced C77S and WT HiPIP from *C. vinosum* at REM level. (B) Close-up of the Fe_4S_4 cluster sites in the two structures depicted in panel A.

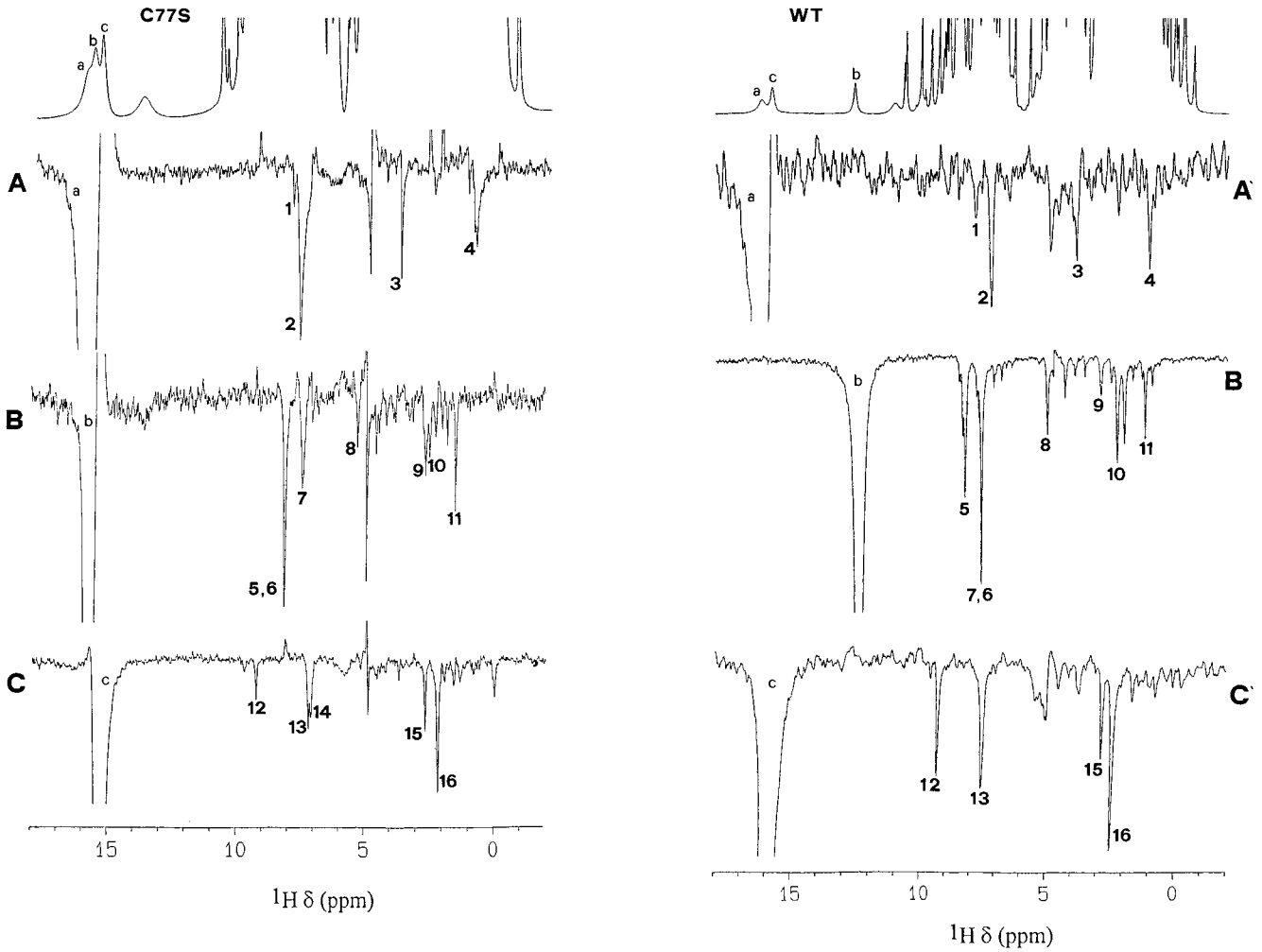

FIGURE 7: ^{1}H NMR spectra (600 MHz, 290 K, pH 5.1 in D_2O) of the reduced C77S HiPIP (left-hand panel) and the reduced WT HiPIP (right-hand panel) from *C. vinosum*: upper traces, reference spectra: lower traces, NOE difference spectra. The latter are labeled according to which signal is saturated: traces A, saturation of signal a (Hβ_2 Cys-43); traces B, saturation of signal b (Hβ_1 Ser/Cys-77); traces C, saturation of signal c (Hβ_2 Cys-63). The assignment of the NOEs is as follows: (1) NH Ala-44, (2) Hβ_1 Cys-43, (3) Hα Val-73, (4) δ-CH_3 Ile-71, (5) Hα Ser/Cys-77, (6) NH Ala-78, (7) Hβ_2 Ser/Cys-77, (8) Hα Tyr-19, (9) Hβ Tyr-19, (10) Hβ Leu-17, (11) δ-CH_3 Leu-17, (12) NH Cys-63, (13) Hδ Phe-66, (14) NH Phe-66, (15) Hβ_2 Phe-66, (16) Hβ_1 Phe-66.

for low-potential Fe_2S_2 ferredoxins [Cheng et al. (1994) and references therein] and for Fe_4S_4 cluster-containing proteins (Kowal et al., 1995).

One of these results that has yet to be fully understood concerns the reduction potentials. In Fe_4S_4 model compounds, substitution of a coordinating sulfur by oxygen either does not affect the redox potential (Weigel & Holm, 1991) or results in a modest increase by 19 mV (Ciurli et al., 1990). In contrast, analogous substitutions in FeS proteins have generally resulted in decreases of reduction potential [between 18 and 72 mV (Cheng et al., 1994; Kowal et al., 1995)].

Comparison of the Structures of the Reduced C77S and WT Proteins. Figure 6A shows a stereo drawing of a best-fit superposition of the average solution structures of the reduced C77S mutant and WT proteins at REM level. For the sake of clarity, only the backbones are shown. The RMSD of the two structures is 0.83 Å for backbone and 1.17 Å for all heavy atoms if residues 3−82 are considered, as was done in the calculations of the above-reported RMSDs within the DG and REM families. Although the backbone RMSD between the C77S and WT structures is higher than the RMSD within the respective DG and REM families of the C77S and WT structures, the core structures of the C77S mutant and WT are very similar, as is clearly seen in Figure 6A.

The highest values of RMSD per residue in this comparison (Figure 3D) are found in the N-terminal region of the protein and are probably due to the additional N-terminal alanine residue of the C77S mutant, which is not present in WT. Since the N-terminus of *C. vinosum* HiPIP is not involved in the formation of elements of secondary structure that could stabilize its position with respect to the rest of the protein, an additional residue may influence its mobility and spatial arrangement. In this context it is interesting to note that the N-terminal $S(\psi)$ values for the REM family of C77S mutant HiPIP are clearly higher than in the case of WT [cf. Figure 7B of Banci et al. (1995)]. If the RMSDs between the two average structures are calculated for residues 14−82 only, the backbone RMSD is 0.69 Å, whereas the RMSD for heavy atoms decreases to a value of 1.10 Å.

Further comparison of the two structures reveals additional maxima of the RMSD per residue values in the sequential stretch Phe-48−Asp-58 and for the amino acids Gln-64−Lys-69 (Figure 3D). The first maximum comprises the already-mentioned external loop and and the poorly defined residue Phe-48; the latter residues are characterized by relatively high RMSD values within the REM family (cf.

Figure 3B,C). The structural significance of these two RMSD maxima in the comparison of the C77S mutant and WT structures cannot be addressed on the basis of the available data.

Figure 6B is a more detailed view of the Fe−S cluster site of both C77S mutant and WT proteins at REM level, showing the high similarity of the protein backbone arrangement around the cluster. Moreover, the side chains of the Fe-coordinating residues are shown; their similar conformations in both C77S and WT proteins, besides being the result of the full procedure for solution structure determination, could be qualitatively anticipated from the resemblance of the 1D NOEs experienced by the hyperfine-shifted β-CH_2 protons of these residues (Figure 7). Thus, the C77S mutation does not significantly alter the protein environment around the cluster.

Concluding Remarks. A complete assignment of the ^{1}H NMR spectra of the C77S mutant of *C. vinosum* HiPIP has allowed us to determine the solution structure of the reduced protein at a level of resolution similar to that of WT. The comparison of the structures shows the extreme similarity of the two proteins. The similarities between the C77S variant and WT proteins extend to the hyperfine shifts of the residues coordinated to the polymetallic center as well as to the NOEs of the Cys77 and Ser77 protons. This applies to both oxidized and reduced forms of the HiPIPs. Overall, this demonstrates that serine can substitute for cysteine without greatly perturbing the electronic structure of the cluster. The reduction potential is also only slightly affected by the substitution, supporting the idea that the polypeptide surrounding the prosthetic group is a very important factor in determining the redox potentials in metalloproteins. It is also demonstrated that serine coordinates to the iron as serinate, despite the much higher pK_a of this residue with respect to cysteine.

Why, then, does nature constantly use cysteines instead of serine in coordinating FeS clusters? One possible answer is the lower thermodynamic stability and/or unfavorable kinetics of cluster formation when serine is used. Variants of *C. vinosum* HiPIP in which any one of the other three cysteines is replaced by serine are considerably less stable than the C77S mutant (unpublished results from our laboratories). The latter protein may only be stable because cluster formation is sufficiently favored by the first three cysteines, and serine simply completes coordination at an already existing polymetallic center. Another reason why the use of serine may not be favored is that oxygen acts as an insulator in electron transfer reactions, as shown by Mizoguchi et al. (1992) using O−S substitutions in blue copper proteins.

ACKNOWLEDGMENT

A.D. thanks the International Centre for Genetic Engineering and Biotechnology for a research postdoctoral fellowship.

SUPPORTING INFORMATION AVAILABLE

Three tables, showing the ^{1}H NMR assignment of the reduced recombinant C77S mutant and of the WT of *C. vinosum* HiPIP and the DIANA library entries of the modified cysteine and serine residues (9 pages). Ordering information is given on any current masthead page.

REFERENCES

Armstrong, F. A., George, S. J., Thomson, A. J., & Yates, M. G. (1988) *FEBS Lett. 234*, 107.

Arseniev, A., Schultze, P., Worgotter, E., Braun, W., Wagner, G., Vasak, M., Kagi, J. H., & Wüthrich, K. (1988) *J. Mol. Biol. 201*, 637−657.

Babini, E., Bertini, I., Borsari, M., Capozzi, F., Dikiy, A., Eltis, L. D., & Luchinat, C. (1996) *J. Am. Chem. Soc. 118*, 75−80.

Backes, G., Mino, Y., Loehr, T. M., Meyer, T. E., Cusanovich, M. A., Sweeney, W. V., Adman, E. T., & Sanders-Loehr, J. (1991) *J. Am. Chem. Soc. 113*, 2055−2064.

Banci, L., Bertini, I., Ciurli, S., Ferretti, S., Luchinat, C., & Piccioli, M. (1993) *Biochemistry 32*, 9387−9397.

Banci, L., Bertini, I., Dikiy, A., Kastrau, D. H. W., Luchinat, C., & Sompornpisut, P. (1995) *Biochemistry 34*, 206−219.

Banci, L., Bertini, I., Ciurli, S., Luchinat, C., & Pierattelli, R. (1995) *Inorg. Chim. Acta 240*, 251−256.

Bartsch, R. G. (1978) *Methods Enzymol. 53*, 329.

Benning, M. M., Meyer, T. E., Rayment, I., & Holden, H. M. (1994) *Biochemistry 33*, 2476−2483.

Bertini, I., Capozzi, F., Ciurli, S., Luchinat, C., Messori, L., & Piccioli, M. (1992) *J. Am. Chem. Soc. 114*, 3332−3340.

Bertini, I., Capozzi, F., Luchinat, C., Piccioli, M., & Vila, A. J. (1994) *J. Am. Chem. Soc. 116*, 651−660.

Bertini, I., Dikiy, A., Kastrau, D. H. W., Luchinat, C., & Sompornpisut, P. (1995) *Biochemistry 34*, 9851−9858.

Breiter, D. R., Meyer, T. E., Rayment, I., & Holden, H. M. (1977) *J. Biol. Chem. 252*, 18660−18667.

Carter, C. W. J., Kraut, J., Freer, S. T., Alden, R. A., Sieker, L. C., Adman, E. T., & Jensen, L. H. (1972) *Proc. Natl. Acad. Sci. U.S.A. 69*, 3526−3529.

Carter, C. W. J., Kraut, J., Freer, S. T., Xuong, N.-H., Alden, R. A., & Bartsch, R. G. (1974) *J. Biol. Chem. 249*, 4212−4215.

Cheng, H., Xia, B., Reed, G. H., & Markley, J. L. (1994) *Biochemistry 33*, 3155−3164.

Ciurli, S., Carrie, M., Weigel, J. A., Carney, M. J., Stack, T. D. P., Papaefthymiou, G. C., & Holm, R. H. (1990) *J. Am. Chem. Soc. 112*, 2654−2664.

Davy, S. L., Osborne, J. M., Breton, J., Moore, G. R., Thomson, A. J., Bertini, I., & Luchinat, C. (1995) *FEBS Lett. 363*, 199−204.

Gaillard, J., Albrand, J.-P., Moulis, J.-M., & Wemmer, D. E. (1992) *Biochemistry 31*, 5632−5639.

Güntert, P., Braun, W., & Wüthrich, K. (1991) *J. Mol. Biol. 217*, 517−530.

Güntert, P., & Wüthrich, K. (1991) *J. Biomol. NMR 1*, 447−456.

Hyberts, S. G., Goldberg, M. S., Havel, T. F., & Wagner, G. (1992) *Protein Sci. 1-I*, 736−751.

Jensen, G. M., Warshel, A., & Stephen, P. J. (1994) *Biochemistry 33*, 10911−10924.

Kowal, A. T., Werth, M. T., Manodori, A., Cecchini, G., Schroeder, I., Gunsalus, R. P., & Johnson, M. K. (1995) *Biochemistry 34*, 12284−12293.

Meyer, T. E., Przysiecki, C. T., Watkins, J. A., Bhattacharyya, A., Simondsen, R. P., Cusanovich, M. A., & Tollin, G. (1983) *Proc. Natl. Acad. Sci. U.S.A. 80*, 6740−6744.

Mizoguchi, T. J., Di Bilio, A. J., Gray, H. B., & Richards, J. H. (1992) *J. Am. Chem. Soc. 114*, 10076−10078.

Mouesca, J. M., Chen, J. L., Noodleman, L., Bashford, D., & Case, D. A. (1994) *J. Am. Chem. Soc. 116*, 11898−11914.

Pearlman, D. A., Case, D. A., Caldwell, G. C., Siebel, G. L., Singh, U. C., Weiner, P., & Kollman, P. A. (1991) *AMBER 4.0*, University of California, San Francisco.

Rayment, I., Wesemberg, G., Meyer, T. E., Cusanovich, M. A., & Holden, H. M. (1992) *J. Mol. Biol. 228*, 672.

Schultze, P., Worgotter, E., Braun, W., Wagner, G., Vasak, M., Kagi, J. H., & Wüthrich, K. (1988) *J. Mol. Biol. 203*, 251.

Szyperski, T., Güntert, P., Otting, G., & Wüthrich, K. (1992) *J. Magn. Reson. 99*, 552−560.

Weigel, J. A., & Holm, R. H. (1991) *J. Am. Chem. Soc. 113*, 4184−4191.

Wüthrich, K. (1986) *NMR of Proteins and Nucleic Acids*, Wiley, New York.

Yoch, D. C., & Carithers, R. P. (1979) *Microbiol. Rev. 43*, 384.

BI9528513